

1 A time domain decentralized algorithm for two channel active noise
2 control

3
4 Somanath Pradhan,^a Guoqiang Zhang and Xiaojun Qiu

5
6 Centre for Audio, Acoustics and Vibration, Faculty of Engineering and IT, University of
7 Technology Sydney, Australia

8
9 **ABSTRACT**

10 Due to their low computational complexity, reduced wiring cost, and flexibility of scaling up,
11 decentralized multiple channel active control systems are attractive in many applications. In a
12 decentralized multiple channel active control system, a number of small subsystems are
13 constructed, which are updated independently with only the associated error signals. In this letter,
14 a time domain two channel decentralized control algorithm is proposed to achieve the similar noise
15 reduction performance as the centralized one. Auxiliary filters are introduced to filter the reference
16 signal for control filter update and a novel design method is proposed to shape the frequency
17 response of the auxiliary filters. The simulation results using the measured impulse responses
18 demonstrate the efficacy of the proposed algorithm for broadband noise control.

19
20
21
22

^a Corresponding Author: Somanath Pradhan (Somanath.Pradhan@student.uts.edu.au)

23 I. INTRODUCTION

24 Active noise control (ANC) technique has gained significant attention in mitigating noise by
25 generating anti-noise using a control algorithm. The filtered-x least mean square (FxLMS)
26 algorithm is the most commonly used algorithm in ANC applications due to its robustness and low
27 computational complexity.^{1,2} To achieve global noise control, a centralized multiple channel ANC
28 system can be employed, which requires many secondary path models for generating the filtered
29 reference signals and all the error signals to update the control filters. When the number of channels
30 increases, the computational complexity of the centralized algorithm increases significantly, and
31 the complexity and cost of wiring and communication overhead between error sensors and the
32 controller cause a big problem.³⁻⁵

33 Many approaches have been proposed to reduce computational complexity of multiple channel
34 systems. Murao *et al.* proposed a mixed-error approach by combining all the error signals into one
35 and used it for centralized control; however, the system possesses high communication load to
36 feed all the error signals to the centralized controller.⁶ Alternatively, a distributed control approach
37 has been proposed by considering each secondary source as a node in a ring network, in which the
38 computational burden is distributed across all the nodes, but at the cost of high transmission
39 bandwidth and delay.⁷

40 Due to their low computational complexity, reduced wiring cost, and flexibility of scaling up,
41 decentralized multiple channel ANC systems are attractive in many applications, in which a
42 number of smaller subsystems are employed to update the control filter independently with only
43 the associated error signal. A study on a two channel frequency domain decentralized ANC
44 (DANC) system shows that the system stability cannot be maintained if the control signals are not
45 constrained in magnitude.⁸ A practical stability condition for decentralized feedback ANC systems

46 has been derived by taking into account the geometrical configuration of secondary sources and
47 error sensors.⁹ It has been found that reducing the number of channels and the distance between
48 secondary loudspeakers and error microphones can increase system stability but at the cost of
49 smaller noise reduction.¹⁰

50 Recently, it is shown that a two channel DANC system can achieve the same noise reduction
51 performance as the centralized one by shaping the eigenvalues of a 2×2 matrix for each frequency
52 bin properly such that they lie on the right complex domain.¹¹ However, it only considers single
53 frequency. An *et al.* proposed a time domain multiple channel DANC system for controlling
54 periodic disturbances recently, but their method has two limitations.¹² First, N nonlinear equations
55 are required to be solved to shape the eigenvalues of an $N \times N$ matrix for each frequency, which
56 remains an open problem without knowing whether a solution exists or not; second, when
57 converting the solution from frequency to time domain, the design of the auxiliary filter to filter
58 the reference signal (to be used in the FxLMS algorithm) is complicated. The sensitive shaping
59 parameters and the filter delay introduced in their system affect the convergence speed of the
60 control algorithm.

61 In this letter, a novel two channel DANC framework in time domain is proposed for
62 controlling broadband noise. Similarly to Ref. 12, the DANC solution in the frequency domain is
63 obtained first and then the optimized time domain algorithm is developed. The novelties of this
64 work are two-fold. First, the genetic algorithm (GA) is employed to compute the DANC solution
65 in the frequency domain, where different frequency bins can have different convergence behaviors
66 with the steepest descent algorithm.¹³ The solution obtained from the GA undergoes a scaling
67 process so that different frequencies have roughly the similar convergence behaviors, which is
68 crucial for broadband control. Second, a new and simple FIR filter design method is adopted for

69 designing the auxiliary filters. The simulation results using the measured acoustic paths
70 demonstrate the effectiveness of the proposed algorithm.

71 **II. THE PROPOSED ALGORITHM**

72 **A. Framework description**

73 Table I shows the framework of the proposed time domain two channel decentralized algorithm.
74 The first step is to find a DANC solution in the frequency domain. To do so, a 2×2 frequency
75 response matrix \mathbf{S} of the secondary paths is constructed and then the GA is employed to obtain the
76 diagonal matrix \mathbf{C} of the DANC for each frequency. In principle, different step sizes can be used
77 for controlling different frequency disturbances using the frequency domain steepest descent
78 algorithm, whereas a single step size has to be used in full band time domain DANC algorithm.
79 This poses a challenge in the system design. As described later, it is necessary to scale the \mathbf{C}
80 matrices to compensate for the different convergence behaviors across the frequencies. After that,
81 the auxiliary FIR filters for filtering the reference signal are designed based on the obtained scaled
82 \mathbf{C} matrices.

83

84 **TABLE I.** Procedure of the proposed algorithm.

Step 1:	Construct a 2×2 frequency response matrix \mathbf{S} of the secondary paths for each frequency.
Step 2:	Shape eigenvalue in frequency domain by finding a diagonal matrix \mathbf{C} using the GA so that the eigenvalues of \mathbf{CS} are at right complex domain.

-
-
- Step 3: Scale \mathbf{C} for each frequency using Eq. (4) and (5) to balance the different convergence behaviors across the frequency bins.
- Step 4: Design the auxiliary FIR filter $R_i(z)$ using Eq. (7).
- Step 5: Carry out the control operation by updating the control filters using Eq. (8).
-

85

86 **B. Eigenvalue shaping in frequency domain**

87 Shaping eigenvalue with the GA is the second step. Following the same iterative learning rule for
 88 a two channel decentralized controller for each frequency, the input to the control sources can be
 89 computed iteratively as⁸

$$90 \quad \mathbf{y}(k+1) = \mathbf{y}(k) - [\mathbf{I} - \mu\mathbf{CS}]\mathbf{y}(k) - \mu\mathbf{C}\mathbf{p}, \quad (1)$$

91 where $\mathbf{y}(k)$ is the input to control source at iteration k , \mathbf{p} represents the primary disturbances at
 92 the error sensors, \mathbf{I} is the identity matrix, μ is the step size, $\mathbf{C} = \text{diag}([c_1, c_2])$, which is to be
 93 obtained, \mathbf{S} denotes the 2×2 frequency response matrix of the secondary paths. To design a
 94 controller that achieves the optimal noise reduction performance, the stability condition is that the
 95 real part of the eigenvalues of the matrix \mathbf{CS} must be positive.¹¹ The diagonal matrix \mathbf{C} can then
 96 be optimized to push the eigenvalues of \mathbf{CS} to the right complex domain.

97 When $\mathbf{C} = \mathbf{S}^H$, Eq. (1) represents the updating equation for the centralized controller. On the
 98 other hand, when $\mathbf{C} = \mathbf{S}_d^H$ (\mathbf{S}_d^H is a diagonal matrix formed by taking the diagonal elements of \mathbf{S}),
 99 Eq. (1) represents the updating expression for the conventional DANC. In the following paragraph,
 100 the GA is used to shape the eigenvalues of \mathbf{CS} appropriately to be at the right complex domain.¹⁴
 101 To do so, the optimization for \mathbf{C} can be formulated as

102
$$\mathbf{C}^* = \arg \min_c 1 \quad \text{subject to } \mathbf{C} = \text{diag}\{c_1, c_2\}$$

103
$$\text{and } \lambda_{i,\text{Re}}(\mathbf{CS}) > 0, \quad i=1,2 \tag{2}$$

103 where 1 and $\lambda_{i,\text{Re}}(\cdot)$ denote a constant function and real part of the i th eigenvalue, respectively.
104 Because it is difficult to apply the GA directly to solve Eq. (2), the above optimization problem
105 has to be reformulated so that the objective function is differentiable. To start, \mathbf{C} is assumed to be
106 a product of two diagonal matrices and can be expressed as $\mathbf{C} = \text{diag}\{\mathbf{a}\}\mathbf{S}_d^H$. Two functions $\theta_{\max}(a)$
107 $= \max_i \angle \lambda_i(\text{diag}(\mathbf{a})\mathbf{S}_d^H)$ and $\theta_{\min}(a) = \min_i \angle \lambda_i(\text{diag}(\mathbf{a})\mathbf{S}_d^H)$ are defined in the range $[-\pi \pi]$. Thus,
108 the optimization problem can be reformulated as

109
$$\mathbf{a}^* = \arg \min_a \left[(\theta_{\max}(\mathbf{a}))^4 \times 1_{\theta_{\max}(\mathbf{a}) > 0} + (\theta_{\min}(\mathbf{a}))^4 \times 1_{\theta_{\min}(\mathbf{a}) < 0} \right], \tag{3}$$

110 subjected to $b_l \leq |a_i| \leq b_u$ and $0 \leq \angle a_i \leq 2\pi$, where $1_{(\cdot)}$ is an indicator function, b_l and b_u are the
111 positive lower and upper limits of the magnitude of elements of \mathbf{a} . The details for applying the GA
112 to find the solution can be found in Ref. 13.

113 **C. Scaling of C matrices**

114 For a DANC system in the frequency domain, the upper bound of step sizes for different
115 frequencies are different when a steepest descent algorithm is employed, indicating that different
116 frequencies exhibit different convergence behaviors.^{8,11} As the proposed algorithm is implemented
117 in full band time domain, only one step size can be employed to incorporate the whole frequency
118 of interest. To address the step size-inconsistency across the two domains, it is necessary to scale
119 the obtained \mathbf{C} matrices from Subsection II-B to mitigate the effect of the different convergence

120 behaviors. In principle, \mathbf{C} matrices can be scaled such that the resulting DANC system have
 121 roughly the same upper bound of step sizes across the frequencies.

122 Because it is time consuming to tune the scales of the \mathbf{C} matrices manually, we propose to
 123 compute the scales mathematically in the following manner. Let the frequency response of the
 124 auxiliary filters $R_i(\omega)$ ($i = 1, 2$) to be

$$125 \quad R_i(\omega) = \psi(\omega) \hat{C}_{GA,i}^*, \quad i = 1, 2 \quad (4)$$

126 where $\psi(\omega) > 0$ denotes the positive scale for frequency ω , and $\hat{C}_{GA,i}^*(\omega)$ is the i th diagonal element
 127 of the solution for \hat{C}_{GA} . The scale $\psi(\omega)$ is computed as

$$128 \quad \psi(\omega) = \left\| \hat{C}_{GA}(\omega) \mathbf{S}(\omega) \right\|_2 / \left\| \mathbf{S}^H(\omega) \mathbf{S}(\omega) \right\|_2. \quad (5)$$

129 It is found empirically that the expression in Eq. (5) can mitigate the effect of the different
 130 convergence behaviors.

131 **D. Auxiliary FIR filter design**

132 The frequency response of the auxiliary filter can be expressed in a compact form as $R_i(\omega) =$
 133 $\mathbf{F}(\omega) \mathbf{\rho}_i$, where $\mathbf{F}(\omega) = [1, e^{j\omega}, \dots, e^{j\omega(L-1)}]$ is the transform vector and $\mathbf{\rho}_i = [\rho_{i0}, \rho_{i1}, \dots, \rho_{i(L-1)}]^T$ is
 134 the filter coefficient vector. Considering the real and imaginary parts for all the angular frequencies
 135 ω_k ($k = 1, 2, \dots, K$), a linear equation can be constructed from Eq. (4) as

136

$$\begin{bmatrix} \text{Re}(\mathbf{F}(\omega_1)) \\ \vdots \\ \text{Re}(\mathbf{F}(\omega_K)) \\ \text{Im}(\mathbf{F}(\omega_1)) \\ \vdots \\ \text{Im}(\mathbf{F}(\omega_K)) \end{bmatrix} \boldsymbol{\rho}_i = \begin{bmatrix} \text{Re}(\psi(\omega_1)\hat{C}_{\text{GA},i}^*(\omega_1)) \\ \vdots \\ \text{Re}(\psi(\omega_K)\hat{C}_{\text{GA},i}^*(\omega_K)) \\ \text{Im}(\psi(\omega_1)\hat{C}_{\text{GA},i}^*(\omega_1)) \\ \vdots \\ \text{Im}(\psi(\omega_K)\hat{C}_{\text{GA},i}^*(\omega_K)) \end{bmatrix}, \quad (6)$$

137 where $\text{Re}(\cdot)$ and $\text{Im}(\cdot)$ denotes the real and imaginary parts, respectively. Denoting the first matrix
 138 of the left hand side of Eq. (6) as \mathbf{A} and the right hand side of Eq. (6) as vector \mathbf{b} , it can be expressed
 139 as $\mathbf{A}\boldsymbol{\rho}_i = \mathbf{b}$. The optimum solution for $\boldsymbol{\rho}_i$, which is the filter coefficient vector of the i th auxiliary
 140 filter, can be obtained as

141

$$\boldsymbol{\rho}_i = (\mathbf{A}^H \mathbf{A})^{-1} \mathbf{A}^H \mathbf{b}. \quad (7)$$

142 Unlike the auxiliary filter design method reported in Ref. 12, this proposed method does not
 143 include any additional delay in the filter, i.e., the effect of the additional delay on convergence
 144 speed of the control algorithm is mitigated. Here, the length of the auxiliary filter L is the same as
 145 the length of secondary paths L_s .

146 E. The time domain control algorithm

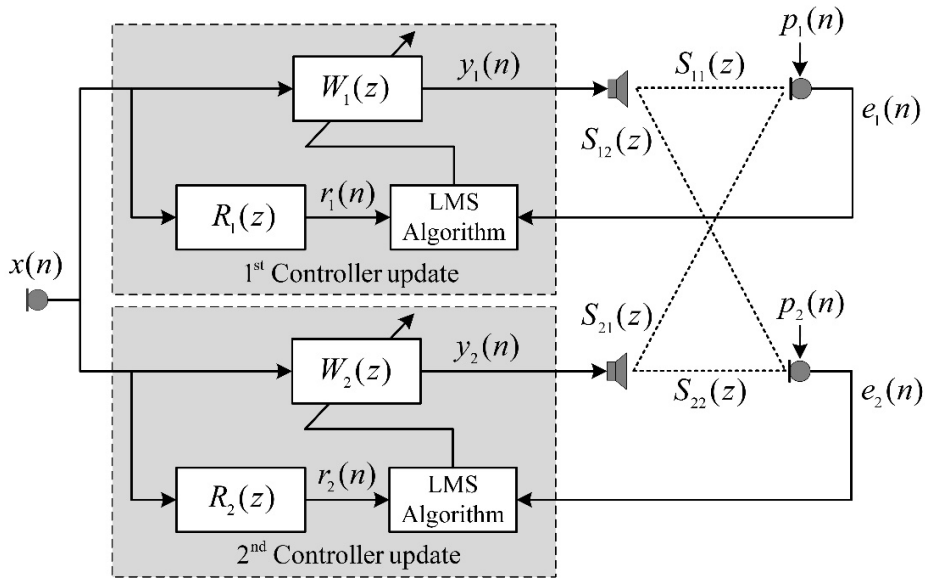
147 Figure 1 depicts the schematic diagram of the proposed algorithm, where $x(n)$ is the reference
 148 signal, $y_i(n)$ is the i th ($i=1, 2$) control signal and $W_i(z)$ denotes the transfer function of the i th
 149 control filter, $p_j(n)$ is the primary disturbance at the j th ($j=1, 2$) error sensor, $S_{ij}(z)$ denotes the
 150 acoustic transfer function from the i th secondary source to the j th error sensor and $s_{ij}(n)$ denotes
 151 its corresponding impulse response and $e_j(n)$ is the residual error signal at the j th error sensor.

152 $R_i(z)$ denotes the transfer function for filtering the reference signal for the i th control filter, the
 153 frequency response of which is optimized based on the GA described in subsection II-B and they
 154 are designed as FIR filters following the procedure described in subsection II-D. Unlike the
 155 conventional DANC system, the reference signal $x(n)$ is filtered through the designed auxiliary
 156 filter $R_i(z)$ and the L_w -tap i th control filter is updated independently with respect to the i th error
 157 signal using the FxLMS algorithm as

$$158 \quad \mathbf{w}_i(n+1) = \mathbf{w}_i(n) - \mu \mathbf{r}_i(n) e_i(n), \quad (8)$$

159 where $\mathbf{w}_i(n)$ is the i th control filter coefficient vector, μ is the step size parameter, and $\mathbf{r}_i(n) = [r_i(n),$
 160 $r_i(n-1), \dots, r_i(n-L_w+1)]^T$ is the tap delayed vector of the filtered reference signal $r_i(n)$ for the i th
 161 control filter with L_w denoting the length of control filter.

162



163

164 Fig. 1. Schematic diagram of the proposed time domain two channel decentralized algorithm.

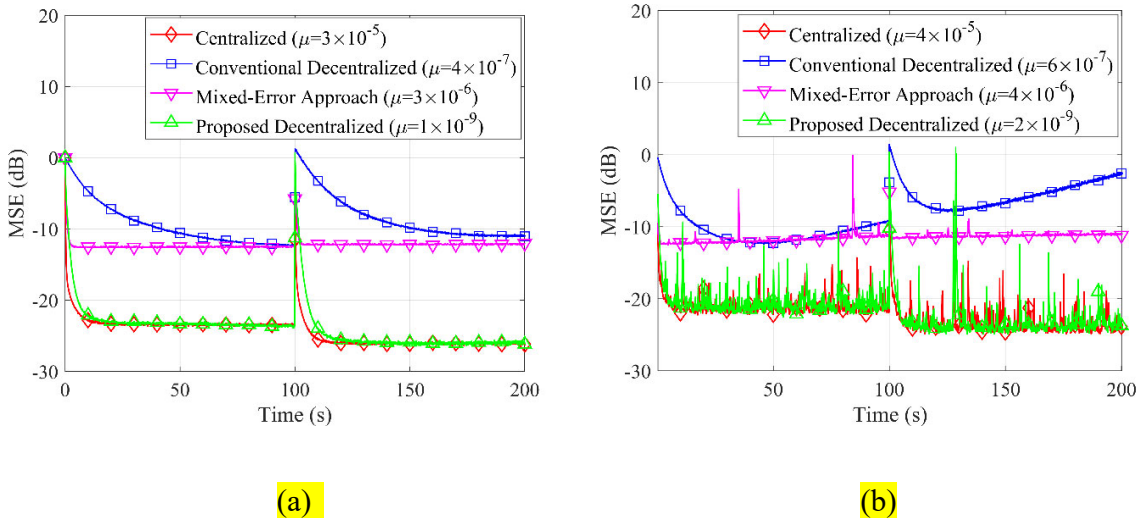
165

166 III. SIMULATIONS

167 In this section, simulations are carried out to demonstrate the noise reduction performance of the
168 proposed algorithm as compared to the conventional time domain decentralized FxLMS algorithm,
169 the centralized FxLMS algorithm, and the mixed-error approach reported in Ref. 6. In the
170 simulations, the primary paths and secondary paths are FIR filters of length 256 and 128,
171 respectively, which were measured in a normal room at the Tech Lab of University of Technology
172 Sydney. The space between the centers of the two secondary loudspeakers was 0.1 m; the primary
173 noise source was placed at 1.0 m away from the secondary sources; the distances from the center
174 of the secondary loudspeakers to their respective error microphones was set as 0.1 m. The primary
175 and secondary paths were obtained with a white noise excitation. Each of the control filter $W_i(z)$ is
176 considered as 256-tap FIR. The sampling frequency used in the simulation is 4 kHz. All the
177 simulation results are ensembled over 50 independent trials and smoothed by moving average
178 method using a window of 256 samples. The normalized mean square error (MSE) is used as the
179 metric for comparison.¹²

180 First, the values of $\hat{C}_{GA,i}^*(\omega)$ are obtained from the GA for frequencies ranging from 1 Hz to
181 2000 Hz with an incremental step of 1 Hz and the corresponding scale parameters $\psi(\omega)$ are
182 calculated. The filter for the i th auxiliary filter is obtained as a 128-tap FIR filter ($L=128$). The i th
183 control filter is updated using the i th filtered reference signal and i th error signal following the
184 learning rule in Eq. (8). Two types of noises are considered for the simulation, where the first one
185 is a white noise and the second is a traffic noise recorded from a highway. A white Gaussian
186 measurement noise with signal to noise ratio (SNR) of 40 dB is considered to mimic a practical
187 environment.

188 Figure 2 depicts the normalized MSE curves for a zero-mean white Gaussian noise with unit
 189 variance, where the primary path changes after 100 s. The variation in the primary path was
 190 obtained by shifting the primary noise source by 0.2 m towards the control sources and then rotated
 191 clockwise by an angle of 30° and pointed towards the secondary sources for demonstrating the
 192 tracking performance of the control filters. One can observe from Fig. 2(a) that the conventional
 193 decentralized algorithm with the maximum possible step size $\mu = 4 \times 10^{-7}$ (without stability issue)
 194 achieves a noise reduction of around 11 dB with a slow convergence. A higher value of step size
 195 results in algorithmic divergence for the conventional decentralized algorithm, which can be
 196 observed from Fig. 2(b).



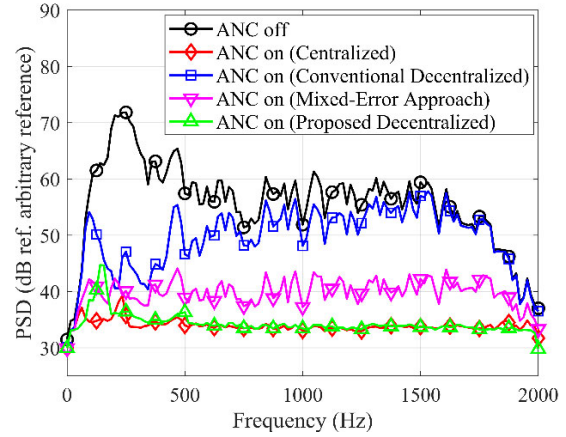
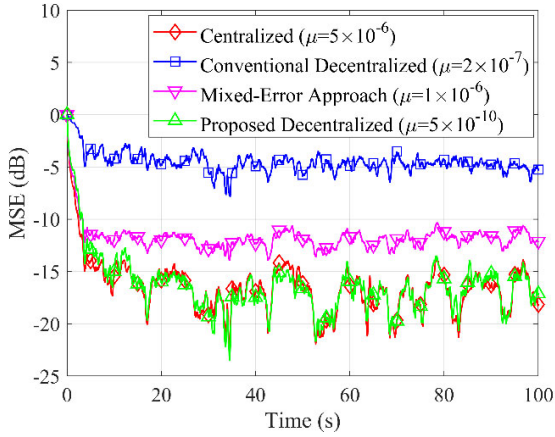
197
 198 (a) (b)
 199 Fig. 2. Normalized MSE curves for zero-mean white Gaussian noise using different algorithms
 200 when they (a) converge and (b) diverge.

201
 202 The proposed decentralized algorithm with its maximum possible step size $\mu = 1 \times 10^{-9}$ achieves
 203 around 23-26 dB noise reduction with a faster convergence speed, whereas the mixed-error
 204 approach with step size $\mu = 3 \times 10^{-6}$ achieves around 12 dB noise reduction, whose control

205 performance is better than the conventional decentralized algorithm but not as good as the
206 proposed algorithm. The centralized algorithm with maximum step size $\mu = 3 \times 10^{-5}$ achieves
207 around 23-26 dB noise reduction with the fastest convergence among the four algorithms. The step
208 sizes of the proposed algorithm and centralized one in Fig. 2(a) are chosen by trial and error in
209 such a way that they achieve similar steady state noise reduction without any stability issue. The
210 step sizes of the conventional decentralized algorithm and the mixed-error approach in Fig. 2(a)
211 are also chosen by trial and error to provide the best possible noise reduction. Higher values of
212 step sizes for the four algorithms compared to the chosen values cause algorithmic divergence or
213 stability issue as shown in Fig. 2(b). It is clear that the upper bound step size for the centralized
214 algorithm is larger than that for the other algorithms.

215 Figure 3 shows the results for the traffic noise recorded from a highway. The normalized MSE
216 curves for this case are depicted in Fig. 3(a), and the power spectral density (PSD) of the sum of
217 two residual error signals with and without control are shown in Fig. 3(b). The conventional
218 decentralized algorithm performs the worst, and the noise reduction performance of the
219 conventional decentralized algorithm deteriorates significantly from 500 Hz to 1500 Hz and there
220 is little control above 1500 Hz. The mixed-error approach is better. The proposed decentralized
221 algorithm and the centralized algorithm perform the best with similar noise reduction. The step
222 sizes of the four algorithms are chosen in the similar way as that for the white noise case. The
223 strength of the proposed algorithm is that each controller only uses its own (nearest) error signal
224 for update, this avoids processing and wiring for other error signals.

225



(a)

(b)

Fig. 3. (a) Normalized MSE curves for traffic noise using different algorithms and (b) the power spectral density with and without noise control.

The proposed algorithm for the two channel DANC requires $4L_w + 2L_s + 2$ multiplications per sample and $4L_w + 2L_s - 4$ additions per sample. Table II presents the computation complexity of the 4 algorithms, and an example is provided for straight forward comparison, where $L_w = 256$ and $L_s = L = 128$. It can be observed that the computational complexity of the proposed algorithm is same as the conventional decentralized algorithm and the mixed error approach, and it is less than its centralized counterpart. In addition to high computational complexity, the centralized ANC system has the highest cost of wiring and the largest communication overhead compared to other algorithms. Despite having vested with reduced complexity, the mixed error approach still needs to communicate with the two error sensors for each control filter update. It is worth noting that the mixed error approach uses mixed secondary path estimates, which are the transfer functions from the i th secondary source to the mixed error signal.⁶ The conventional DANC system and the DANC system with the proposed algorithm require the least cost of wiring and communication overhead; nevertheless, the proposed algorithm requires some preprocessing of the estimated secondary paths

244 before control operation. It is worth noting that the secondary paths are assumed to be perfectly
 245 estimated offline in advance before being used in the algorithm. If the secondary paths change
 246 drastically, re-estimation of secondary paths is required followed by the preprocessing to design
 247 the auxiliary filters. The variation of secondary paths might affect the performance of the system,
 248 which will be investigated in the future.

249

250 TABLE II. Computational complexity per sample of different algorithms.

Algorithms	Multiplication (\times)	Addition (+)	Example	
			(\times)	(+)
Centralized	$6L_w + 4L_s + 4$	$6L_w + 4L_s - 6$	2052	2042
Conventional decentralized	$4L_w + 2L_s + 2$	$4L_w + 2L_s - 4$	1282	1276
Mixed-error Approach	$4L_w + 2L_s + 2$	$4L_w + 2L_s - 4$	1282	1276
Proposed	$4L_w + 2L_s + 2$	$4L_w + 2L_s - 4$	1282	1276

251

252

253 IV. CONCLUSION

254 In this work, a time domain decentralized adaptive control algorithm is proposed for the two
 255 channel ANC system. The frequency responses of the auxiliary filters are optimized using the GA
 256 followed by a scaling process. Unlike the existing methods, a simplified filter design method is
 257 developed. The simulation results with the measured acoustic paths demonstrate that the proposed
 258 algorithm is able to achieve similar noise reduction performance as the centralized algorithm. The
 259 convergence behavior and noise reduction performance of the proposed algorithm is better than
 260 the conventional decentralized algorithm and the mixed-error approach despite having the fact that

261 the upper bound step size for the proposed algorithm is smaller than that for the centralized
262 algorithm. Future work includes extending the proposed algorithm to multichannel ANC systems
263 with large channel number (>2) for broadband noise control.

264

265 ACKNOWLEDGEMENT

266 This work was supported by the Australian Research Council's Linkage Project, grant number
267 LP160100616.

268

269 REFERENCES

270 ¹ S. M. Kuo and D. R. Morgan, *Active noise control systems* (Wiley, New York, 1996).

271 ² S. J. Elliott, *Signal processing for active control* (Academic Press, London, 2001).

272 ³ S. M. Kuo and D. R. Morgan, "Active noise control: a tutorial review," *Proceedings of the IEEE*
273 **87** (6), 943-973 (1999).

274 ⁴ N. V. George and G. Panda, "A particle-swarm-optimization-based decentralized nonlinear
275 active noise control system," *IEEE Trans. Instrum. Meas.* **61** (12), 3378-3386 (2012).

276 ⁵ D. Shi, W.-S. Gan, J. He and B. Lam, "Practical implementation of multichannel filtered-x least
277 mean square algorithm based on the multiple-parallel-branch with folding architecture for large-
278 scale active noise control," *IEEE Trans. Very Large Scale Integ. (VLSI) Systems* (published
279 online 2019).

280 ⁶ T. Murao, C. Shi, W.-S. Gan and M. Nishimura, "Mixed-error approach for multi-channel active
281 noise control of open windows," *Appl. Acoust.* **127**, 305-315 (2017).

282 ⁷ M. Ferrer, M. de Diego, G. Piñero and A. Gonzalez, "Active noise control over adaptive

- 283 distributed networks,” *Signal Process.* **107**, 82-95 (2015).
- 284 ⁸ S. J. Elliott and C. C. Boucher, “Interaction between multiple feedforward active control systems,”
285 *IEEE Trans. Speech Audio Process.* **2** (4), 521-530 (1994).
- 286 ⁹ E. Leboucher, P. Micheau, A. Berry and A. L’Espérance, “A stability analysis of a decentralized
287 adaptive feedback active control system of sinusoidal sound in free space,” *J. Acoust. Soc. Am.*
288 **111** (1), 189-199 (2002).
- 289 ¹⁰J. Tao, S. Wang, X. Qiu and J. Pan, “Performance of an independent planar virtual sound barrier
290 at the opening of a rectangular enclosure,” *Appl. Acoust.* **105**, 215-223 (2016).
- 291 ¹¹G. Zhang, J. Tao, X. Qiu and I. Burnett, “Decentralized two-channel active noise control for
292 single frequency by shaping matrix eigenvalues,” *IEEE/ACM Trans. Audio Speech Lang.*
293 *Process.* **27** (1), 44-52 (2018).
- 294 ¹²F. An, Y. Cao and B. Liu, “Optimized decentralized adaptive control of noise and vibration for
295 periodic disturbances,” *J. Acoust. Soc. Am.* **144** (4), EL275-EL280 (2018).
- 296 ¹³G. Zhang, J. Tao and X. Qiu, “Empirical Study of Decentralized Multi-Channel Active Noise
297 Control Based on the Genetic Algorithm,” in *proceedings of the 23rd International Congress on*
298 *Acoustics*, Aachen, Germany (2019), pp. 6913-6920.
- 299 ¹⁴D. E. Goldberg, *Genetic algorithms*. (Pearson Education India, 2006).

300